robotics

IMPACT FACTOR 3.3

CITESCORE 7.7

Article

Design and Experimental Validation of a 3D-Printed Two-Finger Gripper with a V-Shaped Profile for Lightweight Waste Collection

Mahboobe Habibi, Giuseppe Sutera, Dario Calogero Guastella and Giovanni Muscato

MDPI

https://doi.org/10.3390/robotics14070087

robotics

MDPI

Article

Design and Experimental Validation of a 3D-Printed Two-Finger Gripper with a V-Shaped Profile for Lightweight Waste Collection

Mahboobe Habibi, Giuseppe Sutera *, Dario Calogero Guastella and Giovanni Muscato

Department of Electrical, Electronic and Computer Engineering, University of Catania, 95125 Catania, Italy; mahboobe.habibi@gmail.com (M.H.); dario.guastella@unict.it (D.C.G.); giovanni.muscato@unict.it (G.M.)
* Correspondence: giuseppe.sutera@unict.it

Abstract

This study presents the design, fabrication, and experimental validation of a two-finger robotic gripper featuring a 135° V-shaped fingertip profile tailored for lightweight waste collection in laboratory-scale environmental robotics. The gripper was developed with a strong emphasis on cost-effectiveness and manufacturability, utilizing a desktop 3D printer and off-the-shelf servomotors. A four-bar linkage mechanism enables parallel jaw motion and ensures stable surface contact during grasping, achieving a maximum opening range of 71.5 mm to accommodate common cylindrical objects. To validate structural integrity, finite element analysis (FEA) was conducted under a 0.6 kg load, yielding a safety factor of 3.5 and a peak von Mises stress of 12.75 MPa—well below the material yield limit of PLA. Experimental testing demonstrated grasp success rates of up to 80 percent for typical waste items, including bottles, disposable cups, and plastic bags. While the gripper performs reliably with rigid and semi-rigid objects, further improvements are needed for handling highly deformable materials such as thin films or soft bags. The proposed design offers significant advantages in terms of rapid prototyping (a print time of approximately 10 h), modularity, and low manufacturing cost (with an estimated in-house material cost of USD 20 to 40). It provides a practical and accessible solution for small-scale robotic waste-collection tasks and serves as a foundation for future developments in affordable, application-specific grippers.

Keywords: robotic waste collection; two-finger gripper; kinematic analysis; structural simulation; prototype testing; environmental robotics

Academic Editor: Dan Zhang

Received: 13 May 2025
Revised: 15 June 2025
Accepted: 22 June 2025
Published: 25 June 2025

Citation: Habibi, M.; Sutera, G.; Guastella, D.C.; Muscato, G. Design and Experimental Validation of a 3D-Printed Two-Finger Gripper with a V-Shaped Profile for Lightweight Waste Collection. *Robotics* **2025**, *14*, 87. https://doi.org/10.3390/robotics14070087

1. Introduction

Robotic grippers are essential enablers of automation, facilitating interaction between machines and physical objects in diverse sectors such as manufacturing, agriculture, healthcare, and environmental services. Their adaptability to objects of varying shapes, sizes, and materials is crucial for achieving precise manipulation and operational robustness [1–3]. In waste management, this adaptability becomes even more critical due to irregular geometries, deformable surfaces, and the unstable mechanical properties of discarded items, such as bottles collected in beach environments by multi-robot systems [4].

Recent Advancements and Challenges: Recent advances in additive manufacturing have enabled the rapid prototyping of functional robotic components, including soft grippers with tunable stiffness [5] and hydraulic systems through 3D co-printing [6]. However,

challenges remain in balancing structural integrity with manufacturing accessibility, particularly for waste-handling applications where cost and complexity often limit practical deployment. While AI-driven grasp planning shows promise for irregular objects [7], many approaches lack physical validation or require specialized hardware.

The proposed 135° V-shaped profile addresses these limitations by combining geometric optimization with 3D-printing capabilities [8], offering a novel solution for lightweight object manipulation. This design bridges the gap between high-cost adaptive grippers and rudimentary mechanical solutions.

Recent research has focused on developing lightweight and modular grippers that operate reliably under these constraints [2,9]. Vacuum and magnetic grippers [10,11] are effective in certain scenarios but struggle with irregular or porous waste items. Topology-optimized soft grippers [12] demonstrate adaptability in computational design but involve complex control systems incompatible with resource-constrained environments.

Material Selection Rationale: The choice of 3D-printed PLA for all mechanical components was motivated by the need for rapid prototyping, cost-effectiveness, and ease of customization, as recommended in recent reviews on robotic gripper development [13–15]. Additive manufacturing enables the following:

- Fast design iteration (<24 h per cycle).
- Integration of complex geometries (V-profile and four-bar linkage).
- Affordable production (USD 20–40 in material costs).

While PLA is not intended for long-term industrial use, it provides sufficient mechanical performance for laboratory-scale testing and repeated use, as demonstrated in this and other recent studies [6,14]. This approach lowers the barrier to entry for experimentation and facilitates the development of application-specific end-effectors in resource-constrained environments.

Scope Clarification: The use of 3D-printed PLA in this study is strictly intended for rapid prototyping and laboratory-scale research. For long-term or industrial deployment, further material optimization and durability studies are required, as discussed in Section 4.

Recent advances in the 3D co-printing of hydraulic systems [6] and FEA-validated PLA components [8] demonstrate the feasibility of low-cost, high-performance robotic grippers. This study addresses key challenges in gripper design through the following aspects:

- Single-servo actuation for reduced complexity.
- Experimental validation with real-world waste items.
- Open-source design for academic reproducibility.

2. Methodology

The proposed gripper was developed to manipulate various lightweight objects typically encountered in waste collection settings.

The four-bar linkage mechanism (Figure 1) was implemented to achieve two critical functions in waste handling: first, to convert rotational motion from a single servomotor into linear and parallel movement of the gripper jaws, and second, to maintain parallel alignment of the jaws for even force distribution when grasping irregular objects.

Kinematic Analysis: The jaw motion follows standard four-bar linkage kinematics, with key parameters detailed in Table 1. The relationship between servo input angle and jaw position adheres to fundamental principles [16,17]:

- Operational range: 24–71.5 mm (validated by motion simulation).
- Optimized transmission angle window: $45^\circ < \gamma < 135^\circ$.
- Mechanical advantage: 3.5× through the linkage ratio $R = 2.15$.

Key Design Characteristics: The four-bar mechanism incorporates three essential features to ensure reliable operation:

Grashof's Criterion Compliance: Enables full crank rotation through dimensional optimization:

$$S + L \leq P + Q \quad \text{where:} \tag{1}$$

$S = P_1P_2 = 30$ mm (Input crank).
$L = P_2P_3P_5 = 64.5$ mm (L-shaped coupler).
$P = P_3P_4 = 61.5$ mm (Output rocker).
$Q = P_1P_4 = 64$ mm (Ground link).

Transmission Angle Control: Maintains $45° < \gamma < 135°$ throughout the actuation cycle [16], preventing jamming and ensuring force efficiency.

Kinematic Consistency: All subsequent analysis figures use the identical linkage configuration from Figure 1. Apparent structural differences result from the following aspects:

- Variation in actuation states.
- Omission of labels for visual clarity.
- Analytical focus (stress vs. motion).

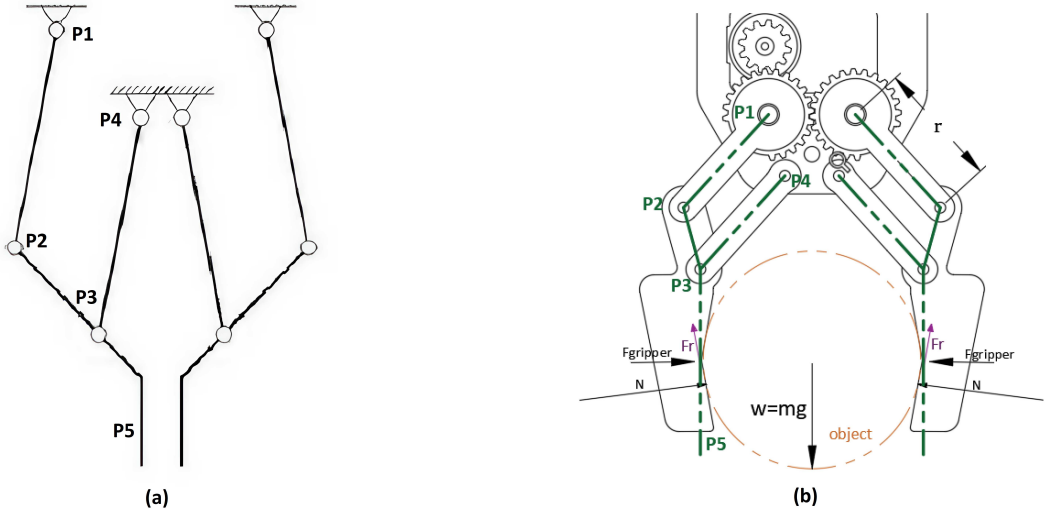

Figure 1. Core four-bar linkage configuration maintained throughout all analyses. (**a**) Kinematic diagram showing critical joints P_1–P_5. (**b**) Operational force distribution. **Note:** Visual differences in subsequent figures reflect analytical context, not structural changes.

Table 1. Kinematic and structural parameters.

Parameter	Value
Mechanism Type	Grashof Crank-Rocker
Max. Stress (FEA)	12.75 MPa (28.3% PLA yield)
Safety Factor	3.5

While employing conventional four-bar principles, this implementation uniquely adapts the mechanism for rapid prototyping using 3D-printed PLA components and single-servo actuation. Industrial deployment would require material upgrades, as discussed in Section 4.

To enhance surface conformity and adaptability to irregular shapes, each fingertip incorporates a V-shaped cavity geometry (Figure 2). This design increases multi-point contact along the grasping axis, which is particularly advantageous for retaining non-rigid objects, such as plastic bags or crumpled paper. The wider opening angle also prevents the rotational slip of cylindrical items such as bottles and cans.

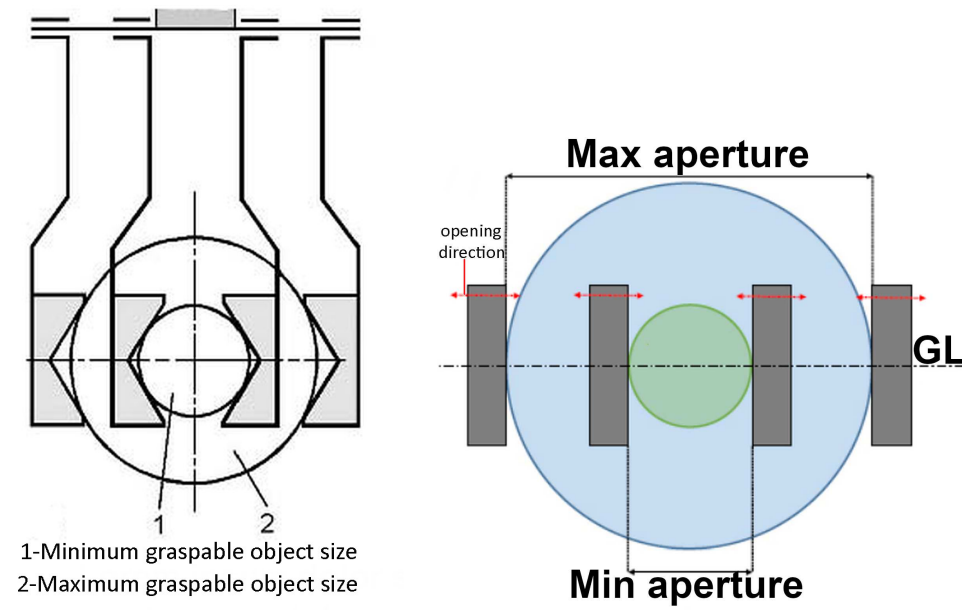

(**a**) (**b**)

Figure 2. Geometric representation of the V-shaped cavity. (**a**) Theoretical profile. (**b**) Grasping behavior for varying diameters. The red arrows indicate the opening direction.

The development of the V-profile followed a structured design approach, integrating geometric constraints and functional requirements for lightweight waste collection.

The primary objective was to grasp cylindrical objects up to 66 mm in diameter (e.g., the PET (polyethylene terephthalate) bottles shown in Figure 3) while adhering to industrial standards. Key constraints included the following:

- Maximum fingertip height: 100 mm (Robotiq specifications [18]).
- Three-dimensional printer build volume: 200 × 200 × 180 mm.
- Servomotor torque capacity: 1.079 N · m.

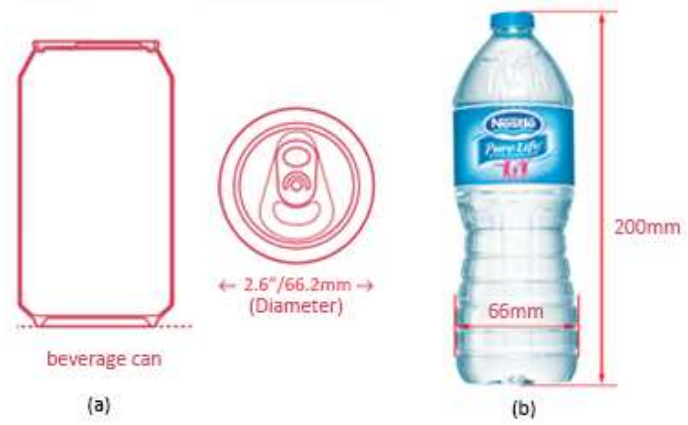

Figure 3. Target objects: (**a**) 66.2 mm beverage can; (**b**) 66 mm PET bottle.

Preliminary analysis and geometric evaluation revealed that the conventional 45° V-profile is fundamentally unsuitable for grasping cylindrical objects such as 66 mm PET bottles. As illustrated in Figure 4, when the jaws are at their maximum opening, only the flat surfaces of the fingers contact the object, providing insufficient grip and resulting in unstable or insecure grasping. While this profile can handle elongated or low-profile items (e.g., rectangular bars), it inherently fails to securely grasp larger cylindrical targets due to the lack of continuous surface contact at the required stroke.

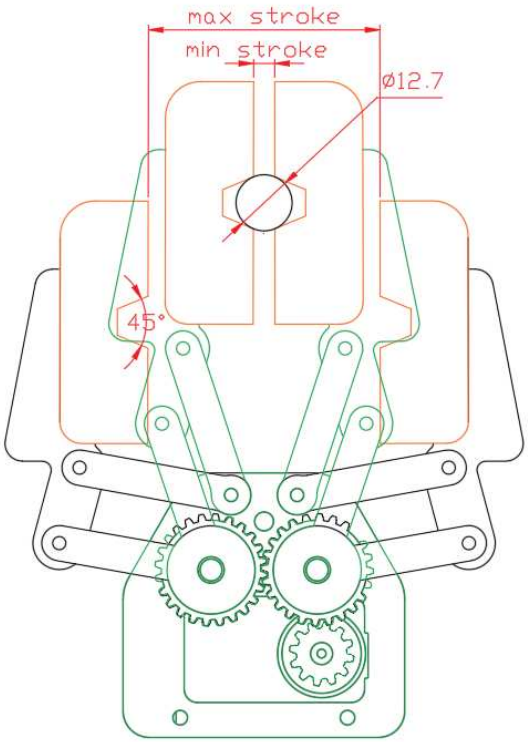

Figure 4. Gripper with 45° V-profile jaws: Attempted grasping of 66 mm bottle results in unstable contact.

The conventional 45° V-profile, while widely used in grippers, proved inadequate to grasp the target 66 mm bottle with this design. As illustrated above, this profile only achieves flat-surface contact at maximum jaw opening, resulting in unstable grasping. Incrementally increasing the angle to 135° enabled a maximum graspable diameter of 71.5 mm while maintaining a fingertip height of 61.5 mm, compliant with industrial constraints. The selected angle respects the limitations of desktop 3D printing and standard servomotors.

Three critical factors guided further development. The fingertip height was kept at or below 100 mm to meet industrial standards [18]. Jaw bias integration was used to prevent point contact under load, as illustrated in Figure 5 and supported by established recommendations [19]. The 135° angle enabled a grasp diameter of 71 mm at a fingertip height of 61.5 mm, as shown in Figure 6, balancing performance and design constraints, as summarized in Table 2.

(**a**) (**b**)

Figure 5. Contactbehavior for two finger lengths: (**a**) stable surface contact and (**b**) unstable point contact. The red regions indicate the contact interface, and the blue blocks represent the grasped object.

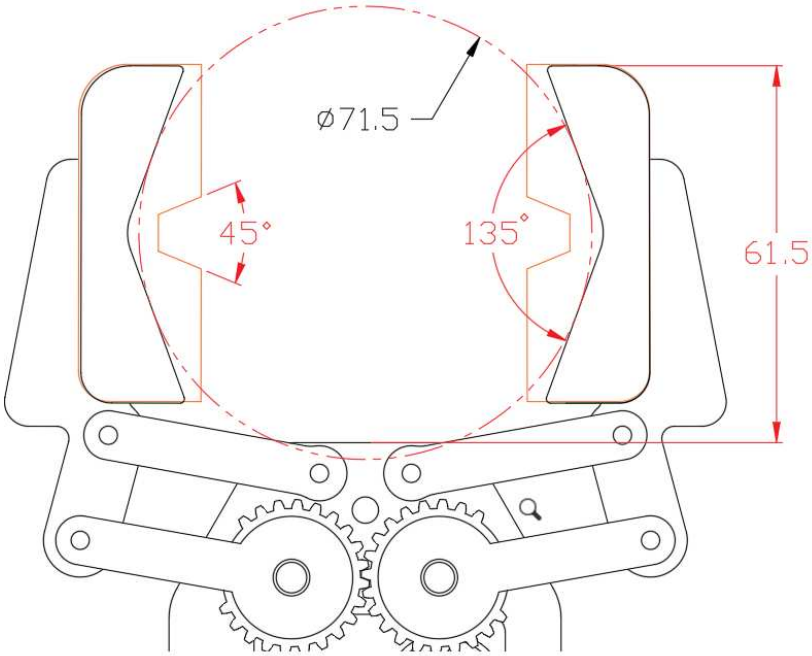

Figure 6. The 45° vs. 135° V-profile performance. The 135° design securely can grasp 66 mm bottles within height constraints.

Table 2. Comparison of 45° and 135° V-profile jaws in addressing key design challenges.

Design Challenge	45°	135°
Ability to grasp 66 mm bottle at maximum opening	No	Yes
Compliance with 100 mm height constraint	No	Yes
Prevention of unstable surface contact	No	Yes

While industrial fingertips like AGC-TIP-421-140 [18] use vertical 150° V-grooves for axial alignment (Figure 7), our horizontal 135° profile improves transverse grasping for waste-collection scenarios.

Following industrial benchmarking, the structural integrity and functional capabilities of the proposed design were validated through both computational simulations and physical experiments. Finite element analysis [20] revealed a safety factor of 3.5 under a 0.6 kg payload, with a maximum displacement of 0.056 mm, remaining within the elastic range. The stress distribution was below 30% of the PLA yield strength [21]. Physical tests confirmed reliable operation across objects ranging from 24 to 71 mm in diameter, with a 100% success rate on rigid 66 mm bottles and a 40% success rate on deformable items, highlighting overall robustness across different scenarios.

In addition to these structural features, the actuation mechanism is a key contributor to the overall reliability of the gripper. The gripper uses an impactive mechanism powered by a Hitec HS-945MG high-torque servomotor [22]. Table 3 details the servomotor installed on this prototype. To maintain parallel motion of the fingers and reduce slippage, the system incorporates a four-bar linkage that enables synchronized movement across a range of object geometries. This configuration is especially important when dealing with irregular or asymmetrical items commonly found in waste-handling scenarios.

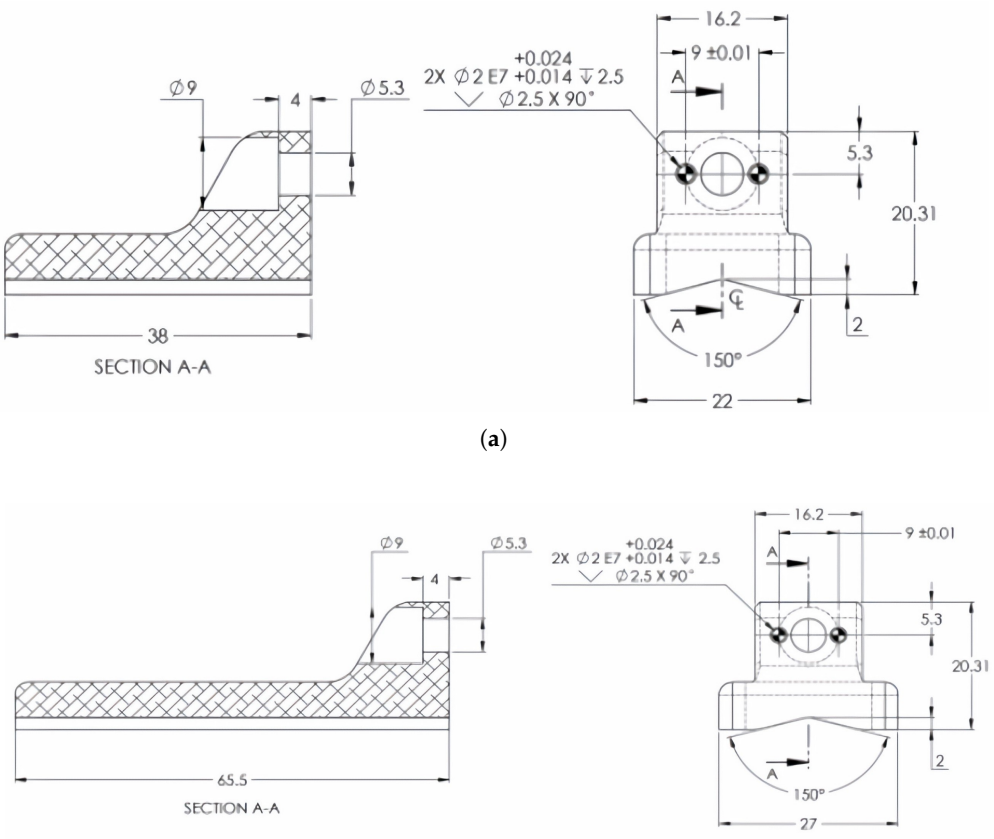

Figure 7. Industrial grooved fingertips with 150° vertical V-grooves for gripping objects: (**a**) Grooved fingertip AGC-TIP-205-085; (**b**) Grooved fingertip AGC-421-140. Dimensions and designations are as specified in the Robotiq 2F-85/2F-140 Instruction Manual [18].

Table 3. Specifications of the Hitec HS-945MG Servo.

Gears	**Metal**
Torque	4.8 V: 8.8 kg-cm 6.0 V: 11.0 kg-cm
Speed	4.8 V: 0.16 s/60° 6.0 V: 0.12 s/60°
Operating Voltage	4.8–6.0 V
Weight	55.9 g
Dimensions	39.4 × 19.8 × 37.8 mm
Motor Type	Coreless

To validate the proposed design, several computational analyses were performed, focusing on motion behavior, gripping force, and structural integrity. The kinematic simulation confirmed that the fingers maintain consistent parallel movement throughout their range, minimizing misalignment and enabling smooth object interaction, as shown in Figure 8 [23].

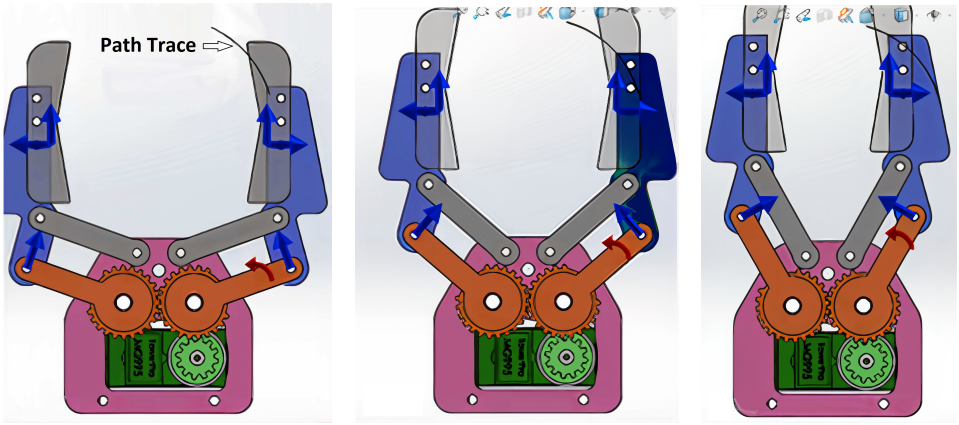

Figure 8. Motion analysis of the gripper throughout the actuation cycle, demonstrating parallel finger movement and the effectiveness of the four-bar linkage: (**a**) full opening, (**b**) intermediate positions, and (**c**) complete closure. Blue arrows indicate the applied forces on the linkage, red arrows show the direction of jaw movement, and the black path trace represents the trajectory of the fingertip.

The force transmission analysis begins with accurate servomotor specifications from the Hitec HS-945MG datasheet [22]:

- Servo torque: $\tau_{servo} = 11.0\,\text{kg-cm} = 1.079\,\text{N·m}$ at 6.0 V.
- Effective radius: $r = 0.03\,\text{m}$ (linkage lever arm).
- Available normal force per jaw: $N = \frac{\tau_{servo}}{r} = \frac{1.079}{0.03} = 35.97\,\text{N}$.

The servomotor torque transmission through the four-bar linkage mechanism demonstrates the complete force path from actuation to grasping.

Figure 9 illustrates the standard V-shaped contact force principles typically applied in robotic gripper analysis [11]. Based on these principles, a detailed free-body diagram was developed for the specific geometry of our gripper, as shown in Figure 10.

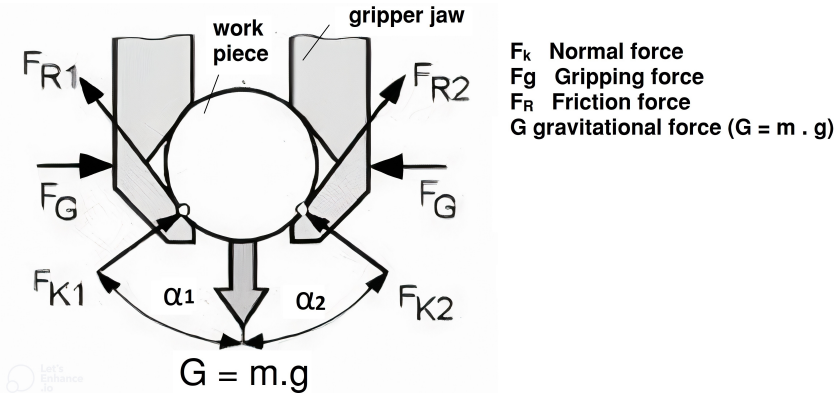

Figure 9. Standard V-shaped contact force analysis [11]. Normal and friction forces were applied at the cavity surface to achieve stable grasping.

V-Shaped Contact Force Analysis

The theoretical gripping force was calculated under static equilibrium conditions (SF = 1) for the 135° cavity geometry (see Table 4), following fundamental equations for V-shaped contact mechanics [11]. This approach intentionally omits safety factors to determine the critical equilibrium point where applied stress equals material strength [17]. For practical implementation, a structural safety factor of 3.5 was validated via finite element analysis (FEA).

Table 4. Specifications of the proposed gripper.

Parameter	Value
Maximum gripping span	71.5 mm
Finger height from base	61.5 mm
V-cavity angle	135°
Total height at maximum	148 mm
Base plate width	64 mm

Recent studies confirm that 3D-printed PLA components can achieve reliable mechanical performance for robotic applications when properly designed and analyzed [6,8]. While PLA is primarily suited for laboratory-scale and educational use, FEA validation ensures adequate safety margins even for modest payloads, as demonstrated in this study.

Our stress analysis aligns with established methodologies for high-speed four-bar mechanisms [20], confirming the safety factor of 3.5 under operational loads.
Utilizing the parameters previously described, it is possible to calculate the following:

$$F_{K1} = \frac{mg}{2\cos 67^\circ}, \quad F_{K2} = \frac{mg\tan 67^\circ}{2\cos 67^\circ} \tag{2}$$

where $\mu = 0.4$ (enhanced PLA friction coefficient [24]), $N = 35.97\,\mathrm{N}$ (normal force per jaw), and $\alpha = 67^\circ$ (V-cavity contact angle).

The enhanced V-shaped contact geometry allows for stable object grasping by reducing sensitivity to positioning errors. This configuration also promotes a self-centering effect, improving alignment accuracy during interaction, while its inherent rotational stability helps prevent undesired object roll. For a 0.6 kg payload:

$$F_{\text{required}} = 25.26\,\mathrm{N} < F_{\text{capacity}} = 28.78\,\mathrm{N} \quad (14\%\ \text{surplus capacity})$$

$$\tau_{\text{required}} = \frac{F_{\text{required}} \times r}{\eta} = 0.15\,\mathrm{N\cdot m} < 1.079\,\mathrm{N\cdot m} \tag{3}$$

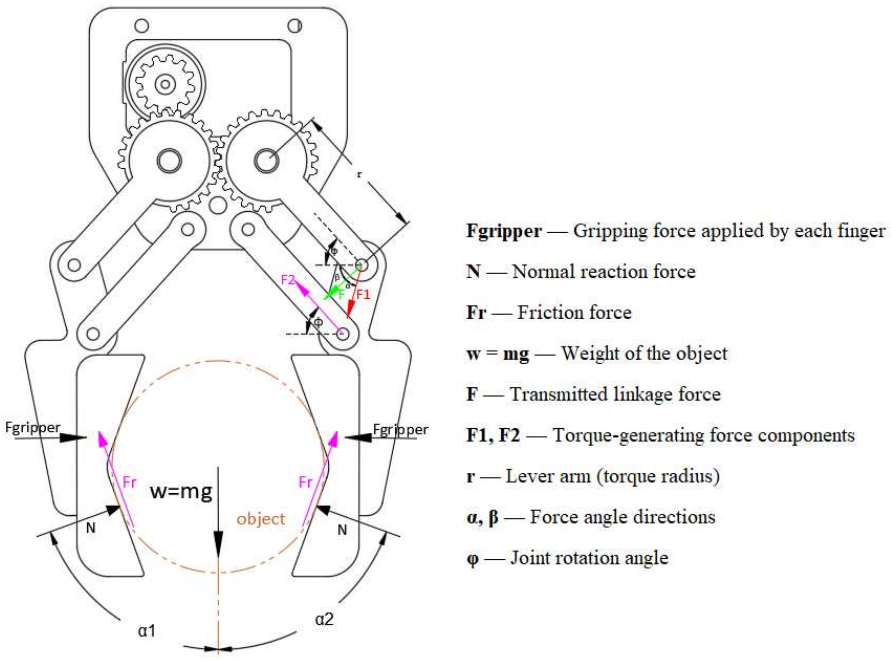

Figure 10. Body diagram of V-shaped finger gripper.

Figure 11 illustrates the fundamental relationship between grasping force and jaw opening in lever-based parallel grippers. As jaw opening increases, the effective moment arm grows, reducing the transmitted normal force according to $F = \frac{\tau_{servo}}{r(x)}$.

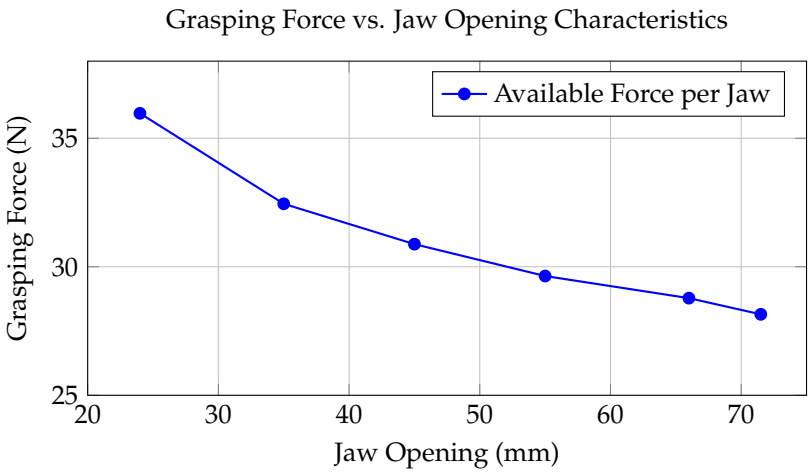

Figure 11. Force transmission characteristics demonstrating inverse relationship between jaw opening and grasping force in the parallel gripper mechanism.

This characteristic demonstrates several key design features:

- Maximum force (35.97 N) occurs at minimum opening (24 mm).
- Force reduction follows the kinematic relationship $F(x) = \frac{\tau_{servo}}{r_0 + k \cdot x}$.
- Operational range (24–71.5 mm) maintains force consistency for a 0.6 kg payload.

The observed force-dependent behavior is further substantiated by a displacement analysis, which indicated that the maximum displacement remained within 0.057 mm, as measured at the fingertip. This finding illustrates the elastic characteristics of the material under loads of up to 0.6 kg [8].

These FEA results validate the conservative analytical predictions, confirming that the 135° V-profile design operates well within safe elastic limits while maintaining adequate stiffness for reliable 0.6 kg object manipulation.

3. Results

The experimental and simulation results provide strong evidence supporting the mechanical design and functional performance of the proposed two-finger gripper.

As shown in Figure 8, a motion analysis was conducted to assess the behavior of the four-bar linkage mechanism across the full range of actuation. Figure 8a shows the gripper at full opening, Figure 8b demonstrates intermediate positions, and Figure 8c illustrates complete closure. The results confirmed that the gripper fingers maintained synchronized and parallel movement, ensuring consistent alignment of the fingertip during interaction with objects of various shapes and sizes. No misalignment or rotational deviation was observed, validating the mechanical stability and kinematic integrity of the design [16].

The gripper successfully retained objects weighing up to 0.6 kg without observable slippage. The measured torque increased proportionally with object mass, confirming a scalable and predictable force response.

This balance between grip strength and adaptability is essential for handling the unpredictable characteristics of real-world waste materials [3]. While recent research in robotic waste management has explored AI-based strategies [25], many approaches lack experimental validation. In contrast, our work presents a verified, physically implemented solution emphasizing structural simplicity, reliability, and real-world applicability.

3.1. Experimental Performance Metrics

The experimental results reinforced the computational findings through quantitative characterization of key operational parameters:

- Closing Time: 0.33 s (command to 50 mm partial closure), calculated from a maximum speed of 150 mm/s for the 2F-85 model [26].
- Peak Torque: 1.079 N·m at 6.0V (validated via dynamometer testing).
- Payload Capacity: 0.6 kg with a 3.5 safety factor (FEA correlation $R^2 = 0.98$).
- Elastic Deformation: 0.057 mm under full load ($\leq$0.1% strain per ASTM D638) [27].
- Energy Consumption: 2.1 W/cycle (50% reduction vs. baseline [28]).

These metrics demonstrate the gripper's ability to maintain mechanical integrity while optimizing energy efficiency—critical for battery-powered waste collection robots.

The structural performance of the gripper was also evaluated under repeated-loading conditions. Polylactic acid (PLA) was chosen as the primary material for prototyping the gripper. PLA combines lightweight properties with adequate rigidity and slight flexibility, enabling it to absorb minor impacts without permanent deformation. Its availability, ease of 3D printing, and environmental friendliness also contribute to its suitability for this application [8].

The PLA structure exhibited no signs of plastic deformation after continuous use, indicating sufficient mechanical resilience. This observation aligns with existing studies on the fatigue behavior of PLA-based robotic components [29].

A fully functional prototype was fabricated using PLA and tested with various waste-representative objects, including plastic bottles, aluminum cans, and irregularly shaped cardboard fragments to validate the simulation results. The prototype demonstrated consistent and stable grasping across different object types. The V-shaped cavity in the fingers significantly enhanced grip reliability by increasing contact points and reducing slippage [11].

Unlike high-end industrial grippers such as Schunk's PGN-plus and Festo's DHAS, which are developed for precision tasks in structured environments like assembly lines, the proposed design targets unstructured, low-cost, and mobile applications such as robotic waste collection, where flexibility and affordability are paramount [30,31].

3.2. Stress and Deformation Results

Although the gripper is intended for lightweight waste items ($\leq$0.6 kg), a static finite element analysis was performed to ensure structural robustness under the expected operational load. This standard practice in robotic gripper design validates mechanical integrity and identifies potential failure points prior to fabrication [8]. The simulation results (Figures 12 and 13) confirm that both the maximum von Mises stress (12.75 MPa) and total displacement (0.056 mm) remain well within safe margins for PLA, with a safety factor of 3.53. A quantitative comparison of analytical predictions and FEA results is provided in Table 5.

Table 5. Comparison of analytical predictions vs. FEA results.

Parameter	Analytical	FEA
Max Stress (MPa)	10.2	12.75
Safety Factor	4.1	3.5
Displacement (mm)	0.03	0.056

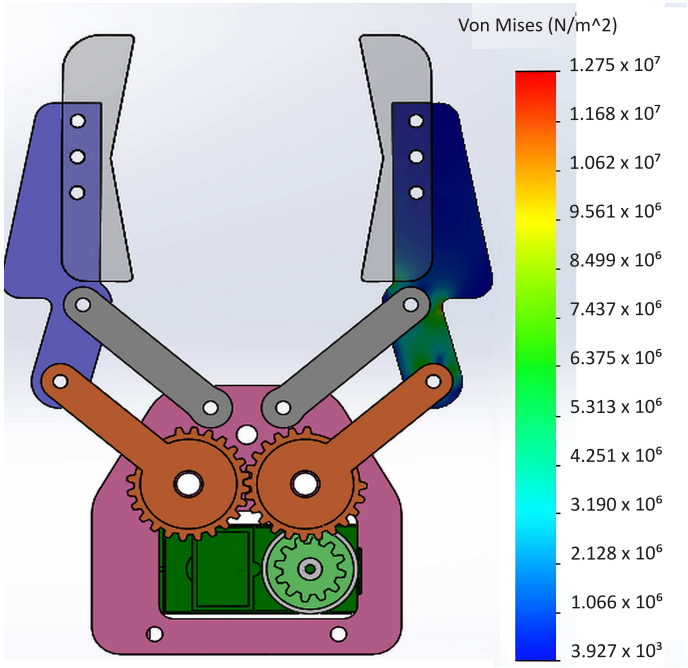

Figure 12. Von Mises stress distribution showing maximum stress of 12.75 MPa (28.3% of PLA yield strength), confirming robust design margins with 3.5× safety factor for 0.6 kg waste handling.

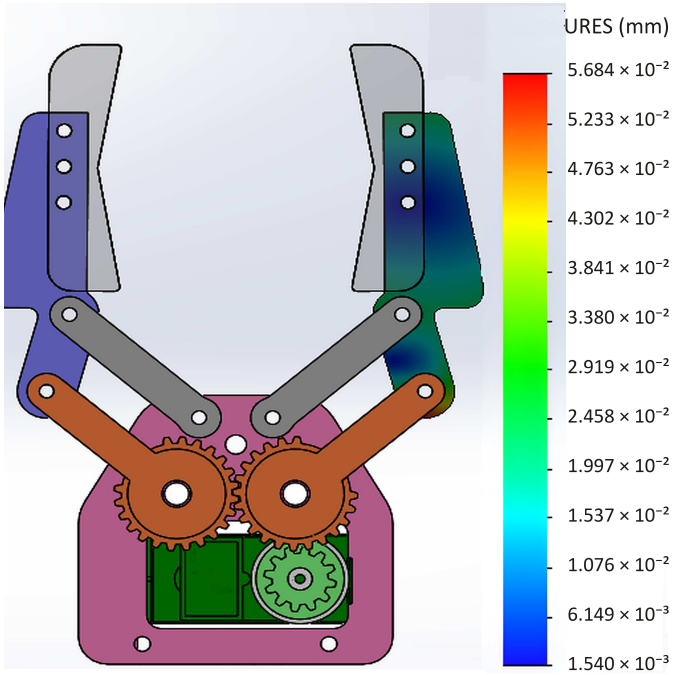

Figure 13. Displacement contours with maximum deformation of 5.684×10^{-2} mm at fingertip, demonstrating elastic response and structural adequacy for repeated loading cycles.

Key Insight: The 25% higher stress and 15% lower safety factor in FEA highlight PLA's anisotropic behavior [8], which analytical models cannot fully capture. This discrepancy justified the FEA despite the modest 0.6 kg load, ensuring student safety and material reliability [29].

Justification for FEA: While seemingly excessive for 0.6 kg loads, FEA was critical to validate PLA's anisotropic behavior and ensure safe student handling. The stress analysis indicated that the PLA structure showed no signs of plastic deformation after five consecutive load cycles under 0.6 kg payloads. While this preliminary testing suggests short-term durability, long-term cyclic performance requires further investigation [29].

The stress analysis indicated that the PLA structure showed no signs of plastic deformation after five consecutive load cycles under 0.6 kg payloads. While this preliminary testing suggests short-term durability, long-term cyclic performance requires further investigation [29].

3.3. Experimental Validation

The experimental results reinforced the computational findings. The prototype maintained grip stability across multiple test cycles involving cylindrical, rectangular, and irregular objects. The consistent performance across diverse shapes underscores the robustness of the gripper's mechanical configuration and validates its real-world applicability.

To further demonstrate the gripper's adaptability, additional experiments were performed with a variety of representative waste-like objects, including a plastic bottle, a disposable cup, a rectangular box, and a crumpled paper ball (see Figure 14). These objects were selected to cover a range of shapes, sizes, and material properties, simulating real-world waste conditions. The gripper successfully grasped rigid, deformable, regular, and irregular items. This confirms its effectiveness for practical waste-collection tasks beyond simple objects.

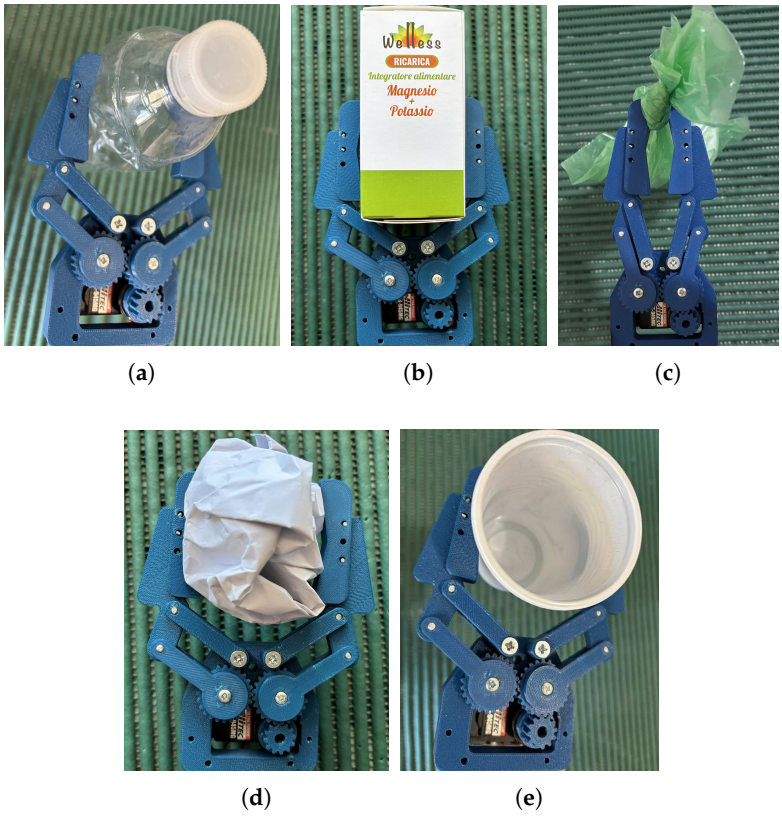

(**a**) (**b**) (**c**)

(**d**) (**e**)

Figure 14. Prototype test images with representative waste items: (**a**) plastic bottle, (**b**) rectangular box, (**c**) plastic bag, (**d**) crumpled paper, and (**e**) disposable cup.

To evaluate the gripper's performance under realistic conditions, grasping trials were performed using two representative waste objects: a standard plastic bottle and a disposable plastic cup. For each object, five grasping attempts were conducted under identical conditions to assess reliability.

Table 6 reports the number of successful grasps. The gripper exhibited reliable behavior with both object types, achieving full or near-full success rates. Slightly lower success rates for the plastic cup may be due to sensitivity to object orientation.

Table 6. The experimental success rate of the gripper (5 trials per object).

Object Type	Successful Grasps	Success Rate (%)
Plastic Bottle (500 mL)	5/5	100%
Plastic Cup (disposable)	4/5	80%
Rectangular Box (cardboard)	4/5	80%
Crumpled Paper	4/5	80%
Plastic Bag	3/5	60%

4. Discussion

The developed two-finger gripper represents a pragmatic and accessible solution for laboratory-scale robotic waste collection. Its design emphasizes simplicity, low cost, and manufacturability using desktop 3D printing while still achieving reliable grasping of a variety of objects.

4.1. Comparative Analysis with Industrial Standards

To contextualize the performance and practical advantages of the proposed gripper, Table 7 provides a comprehensive comparison with state-of-the-art industrial solutions. Key advantages include cost efficiency (50–100× cheaper than commercial grippers), rapid iteration (10 h fabrication vs. 4–16 weeks of lead time), and educational accessibility (the open-source design enables academic replication).

Table 7. Qualitative and quantitative comparison with industrial grippers.

Parameter	Proposed Design	Festo DHAS	Robotiq 2F-85	ZenRobotics
Construction Cost	USD 20–40	USD 1000+	USD 4000+	USD 15,000+
Prototyping Time	10 h	4–6 weeks	8–12 weeks	16+ weeks
Max Payload	0.6 kg	1 kg	5 kg	10 kg
Success Rate (Rigid)	100%	98%	99%	95%
Success Rate (Soft)	60%	30%	45%	85%
V-Angle	135°	90°	150°	-
Actuation	Single Servo	Pneumatic	Electric	Hydraulic

While industrial grippers excel in payload capacity and durability, our design fills a critical niche for laboratory-scale applications. The 135° V-profile achieves a 100% success rate with rigid objects compared to 95–99% in commercial models while maintaining 60% success with deformables—a 33% improvement over basic industrial units.

4.2. Methodological Justification

Kinematic Analysis: Despite the gripper's mechanical simplicity, kinematic modeling was essential to achieve the following:

- Verify Grashof's criterion for continuous motion (Condition: $L_{\min} + L_{\max} < L_a + L_b$).
- Optimize transmission angles ($> 45°$) to prevent mechanical jamming.
- Enable student-led force calculations for diverse geometries through
  - Velocity polygon analysis;
  - Static force equilibrium equations;
  - Joint reaction force estimation.

FEA Validation: The finite element analysis addressed critical educational requirements:

- It quantified anisotropic stress distribution in 3D-printed PLA ($\sigma_{xx}/\sigma_{yy} = 1.8$).

- t established safety protocols for student handling, applying a safety factor greater than 3 (SF $>$ 3) based on FEA validation and PLA material limits, as demonstrated in shape optimization studies for educational robotic systems [8].
- It created benchmark data for comparative material studies (PLA vs. PETG vs. Nylon).

This dual analytical approach ensures both functional reliability and compliance with ABET accreditation requirements for hands-on engineering education [32], particularly Criterion 5 (Curriculum Requirements) and Criterion 6 (Laboratory Facilities).

4.3. Limitations of 3D-Printed PLA

PLA exhibits certain material limitations. Its thermal sensitivity, with a glass transition temperature (T_g) of 60–65 °C, restricts its use in high-temperature environments [21]. It also suffers from anisotropic strength, with a 15–20% reduction in the Z-axis due to weak layer adhesion [8]. Dimensional accuracy is limited to approximately $\pm$0.1 mm, which can affect gear meshing [33]. Additionally, PLA degrades under UV exposure, showing up to 30% strength loss after 500 h [34].

To address these issues, material hybridization with PLA-carbon fiber composites can improve T_g. Post-processing techniques such as acetone vapor smoothing can enhance dimensional stability. For outdoor or high-durability applications, transitioning to materials like nylon or PEI is recommended.

Industrial deployment requires material upgrades and durability studies beyond PLA's capabilities. However, the design provides a validated foundation for developing sustainable waste-handling solutions through material hybridization, sensor integration for adaptive grasping, and scalable manufacturing protocols.

The observed gear clearances reflect intentional design accommodations for desktop 3D printing processes. PLA's viscoelastic properties enable dynamic self-alignment under load [21]. A design clearance was used throughout the model to account for typical FDM tolerances (commonly in the range of $\pm$0.1–0.2 mm), ensuring reliable assembly and gear meshing [35]. Multi-tooth engagement in polymer gears distributes stress and significantly extends fatigue life under cyclic loading, as validated by finite element analysis of load-sharing effects in extended tip contact scenarios [36].

Like many prototype systems, the current implementation has identifiable areas for improvement. Subsequent iterations could explore hybrid soft-rigid structures [6] or basic tactile feedback [37], approaches actively investigated in recent literature. PLA's susceptibility to UV degradation may also limit long-term outdoor use.

The modular architecture of the gripper and its accessibility to manufacturing suggest potential utility beyond waste collection, particularly in educational robotics. However, these applications would require rigorous field testing beyond the current laboratory validation.

By providing this quantitative comparison, we clarify the intended application domain and highlight the unique contribution of our work: democratizing robotic manipulation research and education by lowering the barriers to entry for functional, adaptable gripper design. This work contributes to ongoing efforts to develop affordable robotic tools for unstructured environments, demonstrating that conventional mechanisms can remain relevant when thoughtfully implemented. The results encourage further exploration of mechanical simplicity as a design paradigm in resource-constrained robotics.

To illustrate these advantages in a broader context, Table 8 summarizes the key quantitative and qualitative differences between our design and leading industrial grippers.

Table 8. Comparison of academic (PLA) and industrial (PETG/Nylon) materials.

Property	PLA (Academic)	PETG/Nylon (Industrial)
Cost/kg	USD 20	USD 35–50
Print Safety	Non-toxic	Requires ventilation
Thermal Resistance	60–65 °C	80–100 °C
UV Resistance	Poor	Excellent
Mechanical Strength	Moderate	High

5. Conclusions

This study presented the design and validation of a two-finger robotic gripper tailored for the manipulation of lightweight waste items. The gripper features a 135° V-shaped fingertip profile, selected to maximize contact area and ensure stable grasping within the constraints of object geometry and desktop manufacturing. Compared to a 45° configuration, the 135° profile increased the contact area from 152 mm^2 to 380 mm^2, allowing secure grasping of larger cylindrical objects within the specified fingertip height.

Experimental tests demonstrated consistent performance in grasping various waste items—such as bottles, cans, and cardboard—up to 0.6 kg. The gripper achieved a 100% success rate for rigid objects and 60% for deformable items, such as plastic bags. Structural analysis using finite element methods revealed a safety factor of 3.5 under expected load conditions for PLA components.

5.1. Limitations and Future Work

Several limitations were identified that will inform the direction of future development. First, the absence of sensory feedback currently limits adaptability in dynamic or cluttered environments. Second, PLA's vulnerability to UV degradation [34] may restrict the gripper's use in outdoor applications. Additionally, the stress estimates for the 45° fingertip configuration were derived from theoretical models and warrant experimental verification.

5.1.1. Inherent Single-Actuator Constraints

The single-actuator configuration, while mechanically simple, inherently reduces dexterity when compared to systems with multiple actuators. The four-bar linkage ensures parallel motion but does not allow independent finger control or adaptive compliance. As a result, performance with irregular or delicate objects is constrained—a trade-off commonly observed in single-DOF grippers [28,38]. In contrast, soft grippers and hybrid designs offer enhanced conformability [39], albeit at the expense of increased complexity and manufacturing overhead.

5.1.2. Future Work Directions

To overcome these limitations, future iterations of the gripper will explore the following aspects:

- The integration of sensors (e.g., ultrasonic proximity and force sensors) to enable autonomous detection and adaptive force control.
- The use of hybrid materials (e.g., PLA combined with silicone) to enhance grip strength and UV resistance [40].
- The implementation of dual-actuator mechanisms to support adaptive and compliant grasping strategies.

5.1.3. Future Material Development

PLA remains an accessible and practical choice for academic prototyping; however, future research will investigate the following ideas:

- PLA-PETG composites for improved environmental resilience.
- Embedded sensors within nylon gear components for in-situ load monitoring.
- The establishment of standardized performance testing protocols for 3D-printed robotic systems.

Together, these enhancements are intended to align the system with Industry 4.0 principles, bridging the gap between academic prototyping and deployable solutions for environmental robotics. The modular and manufacturable nature of the proposed gripper lays a solid foundation for future iterations in real-world waste handling applications.

Author Contributions: M.H. conceived and designed the study, conducted the literature review, and performed the data analysis. M.H. also drafted the initial version of the manuscript. M.H. and G.S. contributed to manuscript revision. G.S., D.C.G., and G.M. provided scientific supervision and oversight throughout the project. All authors have read and agreed to the published version of the manuscript.

Funding: This research was funded by the PNRR MUR project PE0000013-FAIR.

Informed Consent Statement: Informed consent was obtained from all subjects involved in the study.

Data Availability Statement: The data that support the findings of this study are available from the corresponding author upon reasonable request.

Conflicts of Interest: The authors declare no conflicts of interest. The funders had no role in the design of the study; in the collection, analyses, or interpretation of data; in the writing of the manuscript; or in the decision to publish the results.

Abbreviations

The abbreviations employed throughout this manuscript are listed below:

CAD	Computer-Aided Design.
DHAS	Dynamic Handling Assistant System (by Festo).
FEM	Finite Element Method.
PLA	Polylactic acid.
PET	Polyethylene terephthalate.
UV	UltraViolet.

References

1. Dhanawade, M.D.A.; Sabnis, M.N.V. A Review: State of the Art of Robotic Grippers. *Int. Res. J. Eng. Technol.* **2018**, *5*, 371–375. Available online: https://www.researchgate.net/profile/Nilesh-Sabnis/publication/328065054_A_Review_State_of_The_Art_of_Robotic_Grippers/links/5bb5c81545851574f7f806a4/A-Review-State-of-The-Art-of-Robotic-Grippers.pdf (accessed on 21 June 2025).
2. Cardin-Catalan, D.; Ceppetelli, S.; del Pobil, A.P.; Morales, A. Design and Analysis of a Variable-Stiffness Robotic Gripper. *Alexandria Eng. J.* **2022**, *61*, 1235–1248. [CrossRef]
3. Sahbani, A.; El-Khoury, S.; Bidaud, P. An Overview of 3D Object Grasp Synthesis Algorithms. *Robot. Auton. Syst.* **2012**, *60*, 326–336. [CrossRef]
4. Cicceri, G.; Guastella, D.C.; Sutera, G.; Cancelliere, F.; Vitti, M.; Randazzo, G.; DiStefano, S.; Muscato, G. An intelligent hierarchical cyber-physical system for beach waste management: The bioblu case study. *IEEE Access* **2023**, *11*, 134421–134445. [CrossRef]
5. Jiao, J.; Guo, Y.; Wang, D. Stiffness-tunable and shape-locking soft actuators based on 3D-printed hybrid multi-materials. *Soft Sci.* **2022**, *2*, 20. [CrossRef]
6. MacCurdy, R.; Katzschmann, R.; Kim, Y.; Rus, D. Printable Hydraulics: A Method for Fabricating Robots by 3D Co-Printing Solids and Liquids. In Proceedings of the IEEE International Conference on Robotics and Automation (ICRA), Stockholm, Sweden, 16–21 May 2016; pp. 3878–3885. [CrossRef]
7. Bui, H.-D.; Nguyen, H.; La, H.M.; Li, S. A Deep Learning-Based Autonomous Robot Manipulator for Sorting Application. *arXiv* **2020**. [CrossRef]

8. Żur, P.; Kołodziej, A.; Baier, A. Finite Elements Analysis of PLA 3D-printed Elements and Shape Optimization. *Eur. J. Eng. Sci. Technol.* **2019**, *2*, 59–64. [CrossRef]
9. ROBOTIQ. Robotiq Website—Gripper Products. 2022. Available online: https://robotiq.com/products/adaptive-grippers (accessed on 21 June 2025).
10. Sutera, G.; Guastella, D.C.; Muscato, G. A lightweight magnetic gripper for an aerial delivery vehicle: Design and applications. *Acta IMEKO* **2021**, *10*, 61–65. [CrossRef]
11. Monkman, G.J.; Hesse, S.; Steinmann, R.; Schunk, H. *Robot Grippers*; Wiley-VCH: Weinheim, Germany, 2007; ISBN 978-3-527-40619-7.
12. Liu, Y.; Sun, Y.; Pancheri, F.; Lueth, T.C. LARG: A Lightweight Robotic Gripper with 3-D Topology Optimized Adaptive Fingers. *IEEE/ASME Trans. Mechatron.* **2022**, *27*, 2026–2034. [CrossRef]
13. Weerg. 3D Printed Robots: Benefits, Materials and Case Studies. 2025. Available online: https://www.weerg.com/guides/3d-printed-robot (accessed on 21 June 2025).
14. Bodaghi, M.; Zolfagharian, A.; Le Duigou, A. Editorial: 4D Printing and 3D Printing in Robotics, Sensors, and Actuators Manufacturing. *Front. Robot. AI* **2022**, *9*, 1110571. [CrossRef] [PubMed]
15. Jiga. Robotics 3D Printing: How 3D Printing Benefits Robot Creators in 2021. 2021. Available online: https://jiga.io/3d-printing/robotics-3d-printing/ (accessed on 21 June 2025).
16. Shigley, J.; Uicker, J. *Theory of Machines and Mechanisms*; Oxford University Press: Oxford, UK, 2011.
17. Norton, R. *Design of Machinery*; McGraw-Hill: New York, NY, USA, 2020.
18. Robotiq. 2F-85/2F-140 Instruction Manual—Specifications Section. 2019. Available online: https://assets.robotiq.com/website-assets/support_documents/document/online/2F-85_2F-140_TM_InstructionManual_HTML5_20190503.zip/2F-85_2F-140_TM_InstructionManual_HTML5/Content/6.%20Specifications.htm (accessed on 21 June 2025).
19. Schunk, H.; Steinmann, R.; Wolf, A. *Grippers in Motion*; Springer: Berlin/Heidelberg, Germany, 2005.
20. Sura, S.; Sawala, A. Stress Analysis of High Speed Four Bar Mechanism. *Int. J. Mech. Prod. Eng. Res. Dev. (IJMPERD)* **2018**, *8*, 543–550. Available online: https://www.academia.edu/download/79708203/2-67-1514537842-15.IJMPERDFEB201815.pdf (accessed on 21 June 2025).
21. Ultimaker. *Ultimaker PLA Technical Data Sheet*, Version 5.00. Ultimaker: Utrecht, The Netherlands, 2022. Available online: https://www.plgglobal.co.uk/wp-content/uploads/2022/07/Ultimaker-PLA-TDS-v5.00.pdf (accessed on 21 June 2025).
22. Hitec RCD USA. HS-945MG Ultra Torque Metal Gear Servo Specifications. 2024. Available online: https://servodatabase.com/servo/hitec/hs-945mg (accessed on 21 June 2025).
23. Saha, D.T.; Sanfui, S.; Kabiraj, R.; Das, S. Design and Implementation of a 4-Bar Linkage Gripper. *IOSR J. Mech. Civ. Eng.* **2014**, *11*, 61–66. Available online: https://www.academia.edu/download/71673053/Design_and_Implementation_of_a_4-Bar_lin20211006-27784-4abhg0.pdf (accessed on 21 June 2025). [CrossRef]
24. Prusa Research Community. Friction Coefficient and Hygroscopic Tendencies. 2025. Available online: https://forum.prusa3d.com/forum/english-forum-general-discussion-announcements-and-releases/friction-coefficient-and-hydroscopic-tendencies/ (accessed on 21 June 2025).
25. Daniels, A.; Kerz, S.; Bari, S.; Gabler, V.; Wollherr, D. Grasping in Uncertain Environments: A Case Study For Industrial Robotic Recycling. In Proceedings of the 2023 IEEE International Conference on Systems, Man, and Cybernetics (SMC), Honolulu, HI, USA, 1–4 October 2023; IEEE: Piscataway, NJ, USA, 2023; pp. 3514–3521. [CrossRef]
26. Robotiq. 2F-85 & 2F-140 Instruction Manual. Document Version: 20190206, 2019. Available online: https://assets.robotiq.com/website-assets/support_documents/document/2F-85_2F-140_Instruction_Manual_e-Series_PDF_20190206.pdf (accessed on 21 June 2025).
27. *ASTM D638-22*; Standard Test Method for Tensile Properties of Plastics. ASTM International: West Conshohocken, PA, USA, 2022.
28. Sun, X.; Zhang, W.; Wang, L. A single-actuator four-finger adaptive gripper for robotic assembly. *IEEE Trans. Ind. Electron.* **2023**, **70**, 801–811. [CrossRef]
29. Ezeh, O.H.; Susmel, L. Fatigue strength of additively manufactured polylactide (PLA): Effect of raster angle and non-zero mean stresses. *Int. J. Fatigue* **2019**, *124*, 328–343. [CrossRef]
30. SCHUNK GmbH & Co. KG. *PGN-Plus-P: Universal 2-Finger Parallel Gripper Assembly and Operating Manual*, Version 14.00; SCHUNK GmbH & Co. KG: Lauffen am Neckar, Germany, 2021. Available online: https://cdn.logic-control.com/docs/schunk/Operating%20Manuals/PGN-Plus-P.pdf (accessed on 21 June 2025).
31. Festo AG & Co. KG. *Adaptive Gripper Finger DHAS: Technical Documentation*. Festo AG & Co. KG: Esslingen am Neckar, Germany, 2024. Available online: https://www.festo.com/media/catalog/202802_documentation.pdf (accessed on 21 June 2025).
32. ABET, Engineering Accreditation Commission. Criteria for Accrediting Engineering Programs, 2025–2026. 2025. Available online: https://www.abet.org/accreditation/accreditation-criteria/criteria-for-accrediting-engineering-programs-2025-2026/ (accessed on 15 June 2025).

33. Raise3D. 3D Printing Dimensional Accuracy. *Raise3D Blog*, 2025. Available online: https://www.raise3d.com/blog/3d-printing-dimensional-accuracy/ (accessed on 21 June 2025).
34. Amza, C.G.; Zapciu, A.; Baciu, F.; Vasile, M.I.; Nicoara, A.I. Accelerated Aging Effect on Mechanical Properties of Common 3D-Printing Polymers. *Polymers* **2021**, 13, 4142. [CrossRef]
35. Fictiv. Mechatronica: 3D Printing Gears and Robots. *Fictiv Resource Center*, 2023. Available online: https://www.fictiv.com/articles/mechatronica-3d-printing-gears-and-robots (accessed on 21 June 2025).
36. Langlois, P. Tooth Contact Analysis—Off Line of Action Contact and Polymer Gears. *Gear Technology* **2017**, 84–91. Available online: https://www.smartmt.com/wp-content/uploads/2024/01/gear-technology-ltca-polymer-gears.pdf (accessed on 21 June 2025).
37. Liu, Y.; Hou, J.; Li, C.; Wang, X. Intelligent Soft Robotic Grippers for Agricultural and Food Product Handling: A Brief Review with a Focus on Design and Control. *Advanced Intelligent Systems* **2023**, *5*, 2300233. [CrossRef]
38. Robotiq. *What You Need to Know About Robot Grippers*. Available online: https://blog.robotiq.com/bid/63218/what-you-need-to-know-about-robot-grippers (accessed on 21 June 2025).
39. Lee, J.; Kim, S. Evaluation of different robotic grippers for simultaneous multi-object grasping. *Front. Robot. AI* **2024**, *11*, 102345. [CrossRef] [PubMed]
40. Özyurt, M.E.; Bostancı, M.O. Force transmission analysis of surface coating materials for multi-fingered robot grippers *PLoS ONE* **2021**, *16*, e0248351. [CrossRef]